1990

The low-angle atomic scattering factors and charge density of zinc

Tabbernor, Mark A.; Fox, Alan G.

Taylor and Francis

Tabbernor, Mark A., and Alan G. Fox. "The low-angle atomic scattering factors and charge density of zinc." Philosophical magazine letters 62.4 (1990): 291-297. http://hdl.handle.net/10945/68402

PHILOSOPHICAL MAGAZINE LETTERS, 1990, VOL. 62, NO. 4, 291–297

The low-angle atomic scattering factors and charge density of zinc

By MARK A. TABBERNOR† and ALAN G. FOX‡

† School of Construction, Engineering and Technology, Wolverhampton Polytechnic, Wulfruna Street, Woverhampton WV1 1SB, England
‡ Materials Science Section, Department of Mechanical Engineering, Naval Postgraduate School, Monterey, California 93943, U.S.A.

[*Received in present form 13 March 1990 and accepted 12 July 1990*]

ABSTRACT

The 0002 and $10\bar{1}3$ low-angle X-ray atomic scattering (form) factors of zinc have been accurately measured by the systematic critical voltage (V_c) method in high-energy electron diffraction. An indication of the value of the $10\bar{1}1$ form factor was also obtained by this technique. These results are in good agreement with recent X-ray *Pendellosung* data for this element and charge difference maps based on this information indicate that bonding in zinc is achieved by the asymmetric depletion of electrons from atomic sites in $\langle 210 \rangle$ directions and redistribution such that there is a maximum build-up of charge density around the mid-point between third nearest-neighbour atoms in the basal plane. This charge distribution is entirely consistent with the long c/a of zinc (1·856), and a comparison with the equivalent charge densities for beryllium ($c/a = 1{\cdot}58$) suggest that there is a simple correlation between bonding mechanism and c/a ratio for these hexagonal elements.

In recent years there have been dramatic improvements in the accuracy to which the atomic scattering factors of elements can be measured experimentally and calculated theoretically. Sato and co-workers and Hart and co-workers (Takama and Sato 1982, Takama, Kobayashi, Hyugaji, Nittono and Sato 1984, Aldred and Hart 1973) have had considerable success in measuring X-ray form factors of elements by X-ray *Pendellösung* techniques, with accuracies as low as 0·1% being achieved. At the same time gamma ray diffraction has also been developed to a stage where it is capable of producing highly accurate X-ray scattering factors (Schneider, Hansen and Kretschmer 1981, Hansen, Schneider and Larsen 1984). In addition, since the late sixties the critical voltage method in high-energy electron diffraction (HEED) has also been used to measure low-angle structure factors in various materials with similar accuracy to the X-ray *Pendellösung* and gamma ray methods; for recent reviews see Fox and Fisher (1988a, 1986). More recently Zuo, Spence and O'Keefe (1988) have used an improved convergent-beam electron diffraction method to determine the low-angle structure factors of GaAs, and they claim a best accuracy of about 0·2%.

Despite the considerable activity by both the theoreticians and experimentalists in producing form factor values for cubic elements very little attention has been focused on h.c.p. metals except for beryllium (Fox and Fisher 1988b, Hansen *et al.* 1984, Dovesi, Angonoa and Causa 1982) where a bonding scheme consistent with its short c/a seems to be well established. This is unfortunate as the electronic basis for bonding and anisotropy in these elements is far from being properly understood. Jones (1978a, b) explored the possibility of using the critical voltage method to measure the low-angle form factors of h.c.p. elements, and the object of the present work is to measure the low-angle X-ray form factors of zinc in this way and to compare the results with the recent

0950–0839/90 $3·00

X-ray *Pendellösung* data of Takama *et al.* (1984) and theoretical calculations of Chakraborty, Manna and Ghosh (1985). It is hoped that this will allow an appraisal of the anisotropy of the electron charge distribution of this metal.

The origin of the critical-voltage effect is as follows. When a crystal that is thick enough for sharp Kikuchi lines to be exhibited (usually 1000 Å or greater) is set at the Bragg reflecting position in HEED, the intensity of the diffracted beam is usually strong owing to the constructive interference of waves scattered in the diffracted beam direction. However, for reflections higher than first order in a systematic row, the diffracted beam intensity can be very small when the accelerating voltage reaches a critical value, V_c. This arises as a result of destructive rather than constructive interference as discussed by Lally, Humphreys, Metherell and Fisher (1972). The critical voltage is very sensitive to the low-order Fourier coefficients of the crystal potential for the systematic row concerned, and hence can be used to measure these and related quantities, such as low-angle form factors, f, with high accuracy. For hexagonal elements the structure factors, F, are given by

$$F^2 = 4f^2 \cos^2 \pi [\tfrac{1}{3}(h+2k)+\tfrac{1}{2}l] \exp(-B \sin^2 \theta/\lambda^2), \quad (1)$$

where h, k and l are the Miller Indices and B the appropriate anisotropic Debye–Waller factor and θ and λ have their usual meanings. If the second- and higher-order form factors and the Debye–Waller for a systematic row are known, then a computer analysis of a critical voltage measurement in that row gives an accurate estimate of the first-order scattering factor.

Computer predictions of the critical voltages in the low-order systematic rows of zinc were made using the free-atom relativistic Hartree–Fock (RHF) form factors of Doyle and Turner (1968) and the room-temperature anisotropic Debye–Waller factors quoted in the International Tables for X-ray Crystallography Volume III (1962), and these are shown in table 1 together with the experimental results. It can be seen that there are seven potentially measurable critical voltages below 3 MeV (the highest voltage electron microscope available) for zinc and that this number drops to four if a conventional 1·0 or 1·5 MeV high-voltage electron microscope (HVEM) is accessible.

Thin samples of zinc for transmission electron microscopy (TEM) were prepared by stamping out 3·0 mm discs from 0·18 mm thick rolled and annealed sheet, and twin jet electropolishing in a Tenupol proprietary electropolisher with a 20% nitric acid : 80%

Table 1. Experimental and theoretical critical voltages for zinc at 293 K (unless otherwise stated).

Systematic row	Reflection minimizing	V_c (theory) (kV)	V_c (experimental) (kV)
$10\bar{1}0$	$30\bar{3}0$	1892	
	$40\bar{4}0$	2810	
0002	0004	180	120 at 118 ± 15 K
	0008	761	not measurable
$11\bar{2}0$	$22\bar{4}0$	2388	
$10\bar{1}1$	$20\bar{2}2$	81	< 80 at 103 K
$10\bar{1}2$	$30\bar{3}6$	3441	
$10\bar{1}3$	$20\bar{2}6$	924	750 ± 20

methanol solution at 20 V and 248 K. The experimental critical voltages shown in table 1 were measured in a JEOL 100CX TEM equipped with a Gatan cooling stage or a Kratos 1·5 MeV HVEM as appropriate. It should be noted that it was not possible to measure the 0008 critical voltage because of the shallowness of the minimization and the weakness of this reflection. The $20\bar{2}2$ critical voltage was found to be significantly below 80 kV at 103 K and attempts to lower the voltage and temperature further to measure V_c proved fruitless. The 0004 critical voltage was measured by the critical-temperature technique of Sellar, Imeson and Humphreys (1980); the voltage was maintained constant at 120 kV and the temperature decreased until the 0004 reflection minimized.

The experimental critical voltages of table 1 were analysed in the usual way (Fox and Fisher 1986) to determine the 0002, $10\bar{1}3$ low-angle X-ray scattering factors of zinc. A lower limit on the $10\bar{1}1$ form factor was also obtained. These are shown in table 2 together with the X-ray *Pendellösung* results of Takama *et al.* (1984) and the theoretical calculations of Chakraborty *et al.* (1985). It should be noted that in the critical-voltage analysis free-atom RHF form factors were used for the higher-angle structure factors and the Debye–Waller factors were taken from the calculations of Merisalo and Larsen (1976) on neutron-diffraction data. On the other hand, Takama *et al.* used temperature factors taken from the single-crystal X-ray work of Skelton and Katz (1968); these are also shown in table 2 and it can be seen that they agree very closely. Appropriate low-temperature Debye–Waller factors obtained from these same sources were used for the analysis of the low-temperature critical voltages.

It can be seen that the experimental results agree with one another within experimental error and in particular there is excellent agreement for the 0002 reflection. It would seen, then, that the X-ray *Pendellösung* experiment has generated a good set of structures factors for zinc, and that these can be used to produce accurate atomic scattering factors. The theoretical calculations of Chakraborty *et al.* (1985) do not closely follow the trend indicated by the experimental results; this is not surprising as they were evaluated using a rather primitive Lowdin α expansion method based on a spherical charge density, which obviously is not applicable to zinc. The calculations of Chakraborty *et al.* are also inadequate for other elements as discussed by Fox, Tabbernor and Fisher (1990).

Table 2. Experimental and theoretical low-angle form factors for zinc.

hkil	$\sin\theta/\lambda$ (Å^{-1})	Takama *et al.* (1984) (experimental)	Present work (experimental)	Chakraborty *et al.* (1985) (theoretical)	Free-atom (RHF)
0002	0·2022	23·58(9)	23·64(7)	24·34	24·19
$10\bar{1}0$	0·2167	23·34(12)		23·75	23·67
$10\bar{1}1$	0·2391	22·50(12)	$<22·78$	22·85	22·87
$10\bar{1}2$	0·2963	20·41(12)		20·70	20·86
$10\bar{1}3$	0·3727	18·17(16)	17·87(14)	18·21	18·29
$11\bar{2}0$	0·3753	18·15(23)		18·14	18·20
0004	0·4043	16·89(4)		17·27	17·28
$11\bar{2}2$	0·4263				16·61
$20\bar{2}0$	0·4333	16·45(7)		16·43	16·41
Room-temperature Debye–Waller factors	B_{33}	2·045(79) Å^2	2·029(40) Å^2		
	B_{11}	0·884(24) Å^2	0·900(24) Å^2		

Fig. 1

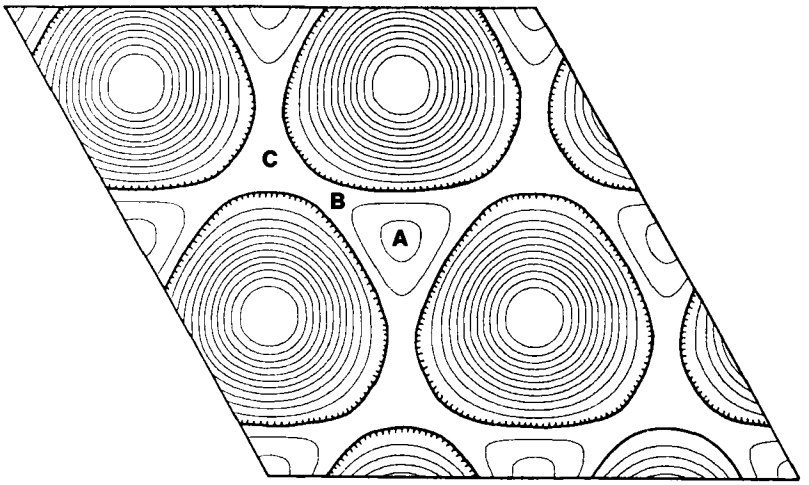

(0001) Charge difference map for zinc as discussed in the text. The zero contours are ticked pointing towards regions of electron depletion and the contour spacing is 0·04 e $Å^{-3}$.

Fig. 2

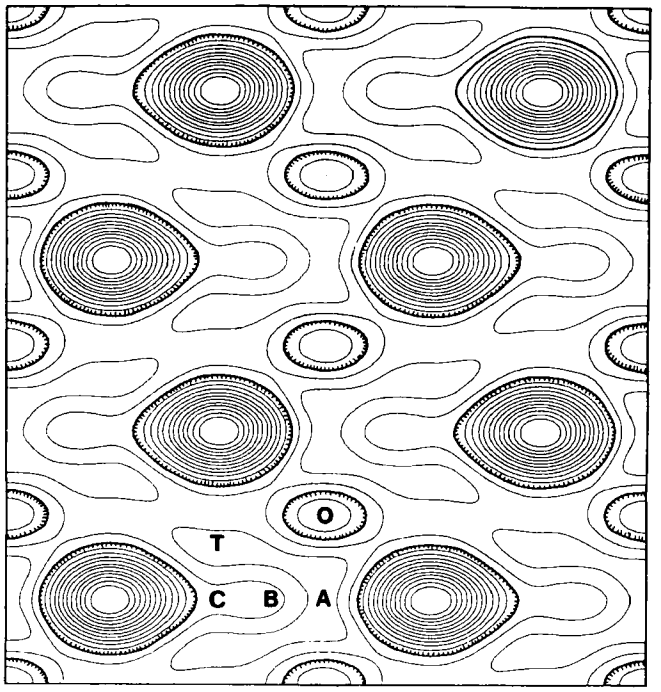

(11$\bar{2}$0) Charge difference map for zinc as discussed in the text. The contour format is as in fig. 1.

Further examination of the data of Takama *et al.* (1984) in table 2 indicates that the higher-angle non-basal crystal structure factors $10\bar{1}3$, $11\bar{2}0$ and $20\bar{2}0$ are close to those of a free atom. This suggests that a charge-difference-density map based on this data will not be severely truncated by the absence of contributions from $11\bar{2}2$ and higher-angle structure factors. Figures 1 and 2 therefore show (0001) (basal) and ($11\bar{2}0$) charge-difference maps calculated from the X-ray *Pendellösung* data of table 2. In these maps the zero contours are ticked towards regions of electron depletion and in the ($11\bar{2}0$) map the octahedral and tetrahedral interstitial sites are marked O and T respectively. The (0001) map shows that bonding in zinc is achieved by the asymmetric depletion of electrons from atomic sites in ⟨210⟩ directions with redistribution such that there is maximum charge build-up in the basal plane at position ($\frac{1}{4}$, $\frac{1}{2}$, 0) in the unit cell (marked A in the figures). The ($11\bar{2}0$) map shows that lobes extend out from these charge density maxima in basal planes into the tetrahedral holes so that the mid-point between nearest-neighbour atoms (position $\frac{1}{2}$, $\frac{1}{2}$, 0) (marked B in the figures) is surrounded by this maximum charge density with lower levels of charge build-up between second-nearest-neighbour atoms. The ($11\bar{2}0$) map also shows that there is a depletion of electron charge from the octahedral holes. These maps indicate that bonding in zinc is highly directional and dominated by nearest-neighbour interactions which are slightly displaced from basal. It is not easy to visualize a simple spd hybrid orbital scheme to account for this, but the bonding is entirely consistent with the long c/a (1·856) for zinc. The asymmetric depletion and build-up of electrons in ⟨210⟩ directions suggests that with appropriate choice of axes the crystal potential is stiffer in the [210] direction than it is in [$\bar{2}10$]. This asymmetry can arise from two sources: (i) vibrational anisotropy due to anharmonic effects or (ii) bonding asphericity. Merisalo, Jarvinen and Kurittu (1978) and Kumpat and Rossmanith (1990) have already detected ⟨210⟩ vibrational anisotropy in the basal plane of zinc from X-ray measurements on higher-angle nearly-forbidden reflections and their results are entirely consistent with those of the present work. However, as pointed out by Takama *et al.* (1984) and shown in table 2, the low-angle form factors for xinc deviate more from free atom (i) as $\sin\theta/\lambda$ decreases and (ii) the closer they

Fig. 3

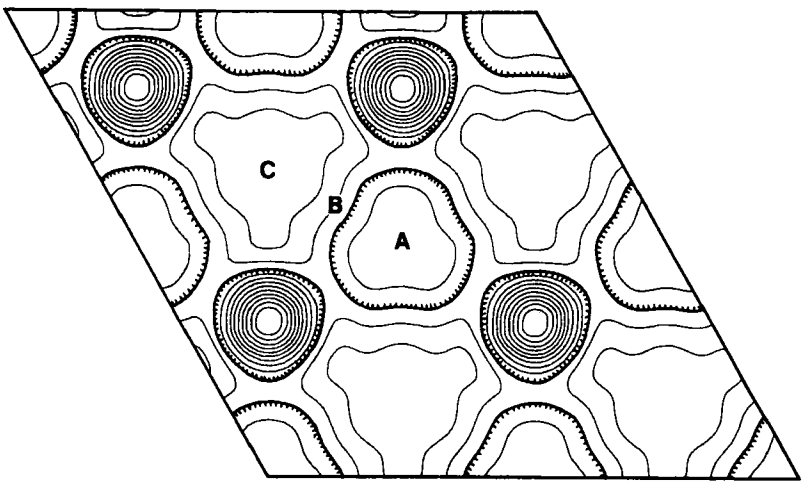

(0001) Charge difference map for beryllium as discussed in the text. The zero contours are ticked pointing towards regions of electron depletion and the contour spacing is 0·02 e Å^{-3}.

Fig. 4

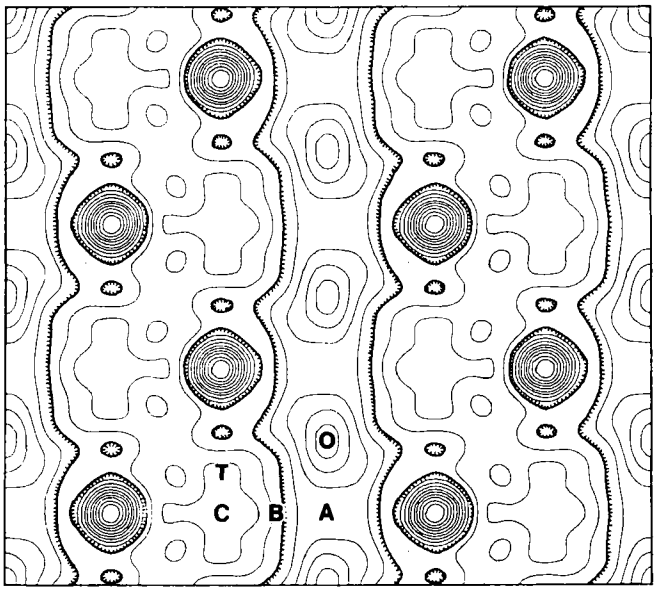

(11$\bar{2}$0) Charge difference map for beryllium as discussed in the text. The contour format is as in fig. 3.

become associated with basal ({000l} planes). This suggests that there is a significant contribution to the ⟨210⟩ atomic site asymmetry from bonding asphericity.

It is interesting and useful to compare these charge difference maps for zinc with the equivalents for beryllium as in this case the bonding is associated with a short c/a (1·58). Figures 3 and 4 thus show the (0001) and (11$\bar{2}$0) charge difference maps for Be based on the band-structure calculated structure factors of Dovesi, Pisani, Ricca and Roetti (1982) corrected for temperature with the Debye–Waller factors of Larsen, Lehmann and Merisalo (1980); the structure factors of Dovesi *et al.* corrected in this way appear to give a good representation of the charge density of beryllium as discussed by Larsen and Hansen (1984) and Fox and Fisher (1988b). The (001) map shows that bonding in beryllium is achieved by asymmetric depletion of electrons in ⟨210⟩ directions but in the opposite sense to zinc. In this case the maximum charge build-up occurs at the ($\frac{1}{2}$, $\frac{1}{4}$, 0) position in the unit cell (marked C in the figures) which is the mid-point between fourth nearest-neighbour atoms in the basal plane (for a short c/a h.c.p. structure) The (11$\bar{2}$0) map for beryllium shows that this maximum charge density extends from the ($\frac{1}{2}$, $\frac{1}{4}$, 0) position out to the tetrahedral holes and there is also build-up between nearest-neighbour atoms. In addition, there is a depletion of electrons from the 'corridor' connecting the octahedral interstitial sites. These charge-difference maps are entirely consistent with the short c/a of beryllium and have been interpreted by Larsen and Hansen (1984) in terms of resonant sp^3 hybrid orbitals. As for zinc the ⟨210⟩ atom site asymmetry appears to arise from both vibrational anisotropy due to anharmonic effects and bonding asphericity. Larsen, Brown, Lehmann and Merisalo (1982) made neutron diffraction studies on several high-angle nearly-forbidden reflections in beryllium and predicted ⟨210⟩ atom site asymmetry due to anharmonic vibrational effects consistent with the present results. However, an examination of the best experimental and theoretical form factors of beryllium discussed previously indicates a well defined form

factor against $\sin\theta/\lambda$ trend which is essentially an inversion of that observed in zinc (i.e. the low-angle form factors associated with (*hki*0) planes deviate more from the free-atom condition than those associated with basal (000*l*), the deviations decreasing as $\sin\theta/\lambda$ increases).

These charge density observations on Be and Zn indicate that bonding in these h.c.p. elements is complex but seems to vary in a simple and predictable fashion with c/a ratio. Both elements exhibit atom-site charge asymmetry in $\langle 210 \rangle$ directions in the basal plane but in an opposite sense according to c/a value. The origin of these charge asymmetries appears to arise from both anharmonic thermal vibrations and bonding asphericity.

ACKNOWLEDGMENTS

This work was supported by a foundation research grant from the Naval Postgraduate School and by the Director, Office of Basic Energy Sciences, Materials Science Division of the United States Department of Energy under Contract DE-AC03-76SF00098. The authors are grateful to Dr K. H. Westmacott of the National Center for Electron Microscopy, Lawrence Berkeley Laboratory, University of California for the use of the Kratos 1·5 MeV HVEM. Thanks are also due to the Director of Wolverhampton Polytechnic for the provision of computing facilities. MAT would also like to thank the U.K. Science and Engineering Research Council for financial support in the form of a studentship and travel and subsistence funds to visit the U.S.A.

REFERENCES

ALDRED, P. J. E., and HART, M., 1973, *Proc. R. Soc. London* A, **332,** 223.
CHAKRABORTY, S., MANNA, A., and GHOSH, A. K., 1985, *Phys. Stat. sol.* (b), **129,** 211.
DOYLE, P. A., and TURNER, P. S., 1968, *Acta crystallogr.*, **24,** 390.
DOVESI, R., ANGONOA, G., and CAUSA, M., 1982, *Phil. Mag.* B, **45,** 601.
DOVESI, R., PISANI, C., RICCA, F., and ROETTI, C., 1982, *Phys. Rev.* B, **25,** 3731.
FOX, A. G., and FISHER, R. M., 1986, *Phil. Mag.* A, **53,** 815; 1988a, *Aust. J. Phys.*, **41,** 461; 1988b, *Phil. Mag.* B, **57,** 197.
FOX, A. G., TABBERNOR, M. A., and FISHER, R. M., 1990, *J. Phys. Chem. Solids* (to be published)
HANSEN, N. K., SCHNEIDER, J. R., and LARSEN, F. K., 1984, *Phys. Rev.* B, **29,** 917.
INTERNATIONAL TABLES FOR X-RAY CRYSTALLOGRAPHY VOL. III, 1962 (Birmingham: Kynoch), p. 237.
JONES, I. P., 1978a, *Phys. Stat. sol.* (a), **47,** 163; 1978b, *Phys. Stat. sol.* (a), **47,** 385.
KUMPAT, G., and ROSSMANITH, E., 1990, *Acta crystallogr.* A, **46,** 413.
LALLY, J. S., HUMPHREYS, C. J., METHERELL, A. J. F., and FISHER, R. M., 1972, *Phil. Mag.*, **25,** 321.
LARSEN, F. K., and HANSEN, N. K., 1984, *Acta crystallogr.* B, **40,** 169.
LARSEN, F. K., LEHMANN, M. S., and MERISALO, M., 1980, *Acta crystallogr.* A, **36,** 159.
MERISALO, M., JARVINEN, M., and KURITTU, J., 1978, *Phys. scripta*, **17,** 23.
MERISALO, M., and LARSEN, F. K., 1976, *Acta. crystallogr.* A, **33,** 351.
SELLAR, J. R., IMESON, D., and HUMPHREYS, C. J., 1980, *Acta. crystallogr.* A, **36,** 686.
SCHNEIDER, J. R., HANSEN, N. K., and KRETSCHMER, H., 1981, *Acta crystallogr.* A, **31,** 711.
SKELTON, E. F., and KATZ, J. L., 1968, *Phys. Rev.* B, **171,** 801.
TAKAMA, T., KOBAYASHI, K., HYUGAJI, M., NITTONO, O., and SATO, S., 1984, *Jap. J. appl. Phys.*, **23,** 11.
TAKAMA, T., and SATO, S., 1982, *Phil. Mag.* B, **45,** 615.
ZUO, Z. M., SPENCE, J. C. H., and O'KEEFE, M., 1988, *Phys. Rev. Lett.*, **61,** 353.